

FINDING BLACK HOLES WITH MICROLENSING

ERIC AGOL¹, MARC KAMIONKOWSKI, LÉON V. E. KOOPMANS, AND ROGER D. BLANDFORD

California Institute of Technology, Mail Code 130-33, Pasadena, CA 91125 USA

Draft version October 27, 2018

ABSTRACT

The MACHO and OGLE collaborations have argued that the three longest-duration bulge microlensing events are likely caused by nearby black holes, given the small velocities measured with microlensing parallax and non-detection of the lenses. However, these events may be due to lensing by more numerous lower-mass stars at greater distances. We find a-posteriori probabilities of 76%, 16%, and 4% that the three longest events are black holes, assuming a Salpeter IMF and $40 M_{\odot}$ cutoff for neutron-star-progenitors; the numbers depend strongly on the assumed mass function, but favor a black hole for the longest event for most standard IMFs. The longest events (> 600 days) have an a-priori $\sim 26\%$ probability to be black holes for a standard mass function. We propose a new technique for measuring the lens mass function using the mass distribution of long events measured with ACS, VLTI, SIM, or GAIA.

Subject headings: black hole physics — gravitational lensing — Galaxy: stellar content

1. INTRODUCTION

Counting the number of black-hole stellar-remnants in our Galaxy is complicated by their faintness. Only a few dozen of an estimated 10^7 – 10^9 black-holes are observed as X-ray binaries (van den Heuvel 1992). Black-hole numbers estimated from stellar-population synthesis are inaccurate due to variations in IMF with metallicity, uncertainty in the star-formation history, and uncertainty in the cutoff mass for neutron-star progenitors. To count the bulk of the black holes (isolated or in wide binaries) requires a different observable signature, the best candidate being gravitational microlensing since it only relies on gravity.

Microlensing events are primarily characterized by the event timescale, $\hat{t} = 2R_E/v$, where R_E is the Einstein radius in the lens plane, $R_E = [4GMc^{-2}D_{Sxy}]^{1/2}$, v is the velocity of the lens perpendicular to the observer-source axis, M is the lensing mass, $D_{L,S}$ are the distances to the lens or source, $x = D_L/D_S$ is the fraction of distance of the lens to the source, and $y = 1 - x$. The motion of the Earth causes magnification fluctuations during long events, an effect called “microlensing parallax” ($\mu - \pi$), allowing one to measure the reduced velocity, $\hat{\mathbf{v}} = (\mathbf{v}_L - x\mathbf{v}_S)/y - \mathbf{v}_{\odot}$ (Gould 1992), where L, S, \odot stand for the lens, source, and Sun and the velocities are perpendicular to the lensing axis. Given D_S and $\hat{\mathbf{v}}$, the lens mass is then solely a function of x ,

$$M(x) = (\hat{v}tc)^2 y / (16Gx D_S). \quad (1)$$

The mass is 0 for $x = 1$, rising to ∞ for $x = 0$, thus to estimate M requires knowing x .

Bennett et al. (2001, hereafter B01) and Mao et al. (2002, hereafter M02) claim that the three longest-duration microlensing events discovered toward the bulge with $\mu - \pi$ measurements are likely black holes. To arrive at this conclusion, they assume that each lens is a member of a population that has a velocity and spatial distribution characteristic of the disk and bulge. Here we in addition

assume that the lenses are drawn from a population that has a *mass function* characteristic of stellar and stellar remnant populations in the disk and bulge, and is independent of x . This latter assumption is not true for young bright disk stars (which do not contain much of the disk mass), but may be true for lower mass stars and compact remnants in the disk and bulge. We then find that the probability that these events are black holes is somewhat reduced.

In §2, we apply the analysis of B01 to MACHO-99-BLG-22 and estimate the implied total black hole number. In §3, we include a mass function in our prior for the lens mass. In §4, we consider the timescale distribution for bulge events and describe how mass measurements of long events may provide an estimate of the lens mass function.

2. MASS ESTIMATE FROM REDUCED VELOCITY ONLY

B01 and M02 present seven microlensing events toward the bulge of the Galaxy with $\mu - \pi$ measurements as shown in Figure 1. These events have greatly decreased χ^2 when the $\mu - \pi$ effect is included and are unlikely to be caused by a binary lens or source. B01 have computed a distance probability for MACHO-96-BLG-5 and MACHO-98-BLG-6 using a likelihood function which depends on the observed reduced velocity and assumes the source is in the bulge. Using equation (1) they find that the most likely masses for the their two longest events are $> 3M_{\odot}$ at 68% confidence. Given that these lenses are not detected as main-sequence stars, they argue that they must be black holes. Using the likelihood function of B01, we find that the mass probability for MACHO-99-BLG-22 (OGLE-1999-BUL-32) has $M = 11_{-6}^{+12} M_{\odot}$ and a 81% probability of being a black hole using the best-fit parameters of Bennett et al. (2002, B02). This differs from the results of B02 due to different assumed disk and bulge velocity dispersions.

If all three events are due to disk black-holes, we can estimate the total number. The detection efficiency, ϵ , for events from 100–400 days is 20% (Alcock et al. 2000),

¹Chandra Fellow, Email: agol@tapir.caltech.edu

which we assume also holds at longer \hat{t} (these events are drawn from the alert sample which have a different selection criterion, so a different ϵ may apply). We have computed the timescale probability for black-hole lensing events, and find that only $\sim 40\%$ have $\hat{t} > 1$ year, so $\epsilon \sim 13\%$. These three events yield $\tau \sim 5 \times 10^{-7}(\epsilon/0.1)^{-1}$, implying $N_{\text{total}} \sim 5 \times 10^8((M)/9M_{\odot})^{-1}(\epsilon/0.1)^{-1}$ disk black holes. This estimate is larger than estimates based upon the expected ratio of black-hole to neutron-star remnants, $\sim 10^8$, (Shapiro & Teukolsky 1983, van den Heuvel 1992) and chemical enrichment by supernovae within the Milky Way, $\sim 2 \times 10^8$ (Samland 1998). This discrepancy indicates that either $\epsilon = 20\%$ is too low, the IMF was much more top-heavy in the past, or the events are due to more distant, low-mass stars. We next explore the third option.

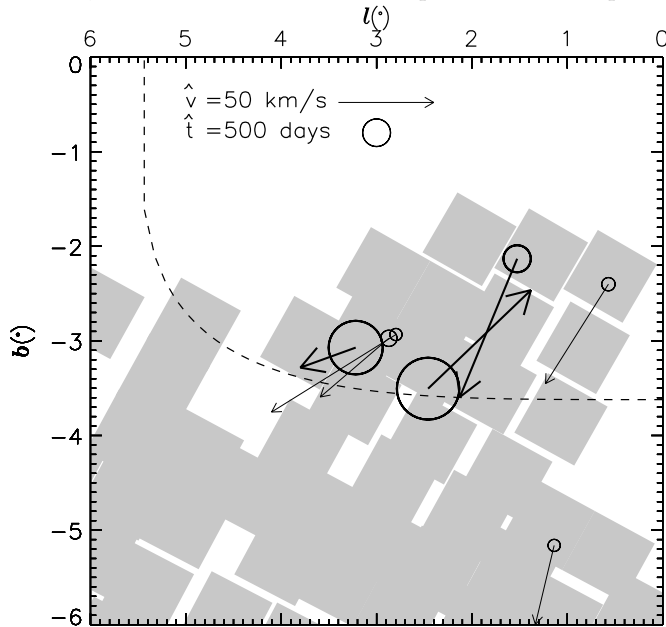


Fig. 1 - The velocity vectors, $\hat{\mathbf{v}}$, and event durations, \hat{t} (proportional to circle size), for seven μ - π microlensing events from B01 and M02. The shaded regions show the MACHO bulge fields, while the dashed line shows the region where the bulge density is half of the central bulge density in the sky plane at the distance of the bulge. Bold-face indicates three black hole candidate events.

3. MASS FUNCTION PRIOR

To recap, the small reduced velocities may indicate that the three longest events most likely lie within 3 kpc and thus should have masses $> 3M_{\odot}$. However, if a lens is more distant, it is less massive (equation 1) and thus drawn from a more abundant population, which can compensate for the small probability of distant lenses to have a small reduced velocity. Here we investigate the mass likelihood given $\hat{\mathbf{v}}$ and \hat{t} using the spatial probability $dn_L/dM = \rho(x)\phi(M)/\langle M \rangle$, where $\phi(M)$ is the mass function of a 10 Gyr-old stellar population (independent of x), $\int \phi(M)dM = 1$, and $\langle M \rangle = \int dM M\phi(M)$ is the mean stellar mass.

To compute $\phi(M)$, we start with the broken power-law IMF from Kroupa (2002), and, following Gould (2000), convert stars with masses $M_{\text{cns}} < M < M_{\text{cwd}}$ into white dwarfs, $M_{\text{cwd}} < M < M_{\text{cns}}$ into neutron stars, and $M_{\text{cns}} < M$ into black holes. We set $M_{\text{cns}} = 1M_{\odot}$ and

$M_{\text{cwd}} = 11M_{\odot}$ (Samland 1998), while we vary M_{cns} . We use Gaussian distributions for the white-dwarf and neutron-star mass functions with $M_{\text{wd}} = 0.5 \pm 0.1M_{\odot}$ (Bragaglia et al. 1995) and $M_{\text{ns}} = 1.35 \pm 0.04M_{\odot}$ (Thorsett & Chakrabarty 1999). Black holes we describe with $\phi_{\text{BH}} \propto M^{-0.5}$ for $3M_{\odot} < M < 15M_{\odot}$, consistent with the measured mass function of black holes in X-ray binaries (which may have a different mass function than isolated black holes). We compute the relative numbers of each compact remnant by varying the high-mass IMF slope $2 < \beta < 3$, where $\phi_{\text{IMF}} \propto M^{-\beta}$, equating the number of each compact remnant with the number of stars in the IMF with appropriate mass range. We assume that this mass function applies in both the disk and bulge.

The number of black holes strongly depends on the slope of the IMF, β , and the maximum neutron-star-progenitor mass, M_{cns} . We choose as a fiducial value the Salpeter $\beta = 2.35$, consistent with the observed IMF (Kroupa 2002), and $M_{\text{cns}} = 40M_{\odot}$, consistent with chemical-evolution models of the Galaxy (Samland 1998). The resulting mass function has mass fractions of 7% in brown dwarfs, 77% in main-sequence stars, 13% in white dwarfs, 1% in neutron stars, and 1.5% in black holes. This corresponds to a total of about 10^9 neutron stars and 2×10^8 black holes in the Milky Way.

Using Bayes' theorem, the likelihood of a lens to be at a given distance, x , for fixed source distance D_S is $\mathcal{L}(x|\hat{t}, \hat{\mathbf{v}}) = \mathcal{L}(\hat{t}, \hat{\mathbf{v}}|x)$ for no prior on the distance and no errors on the timescale and velocity measurements. For a survey of duration T covering a solid angle of Ω , then the solid angle cross section for magnification by $> 30\%$ by a lens with reduced velocity \hat{v} is $2R_E\hat{v}yT/D_L^2$. We must then multiply by the total number of lenses at that distance and integrate over the phase space of the velocity distribution of lenses and sources. We include lenses and sources in the disk and bulge using the bar model described in Dwek et al. (1995) and Han & Gould (1995) and a double-exponential disk with scale length 3 kpc, scale height 325 pc, Galactic center distance 8 kpc, solar circular velocity 200 km/s, velocity ellipsoid $\sigma_z : \sigma_{\phi} : \sigma_r = 1 : 1.3 : 2$, $\sigma_z = 17$ km/s at the solar circle with a scale length of 6 kpc, and asymmetric drift of $\sigma_r^2/120$ km/s (Buchalter, Kamionkowski & Rich 1997). The likelihood function becomes

$$\mathcal{L}(\hat{t}, \hat{\mathbf{v}}|x) = N_S \int dM d\mathbf{v}_{\mathbf{S}} d\mathbf{v}_{\mathbf{L}} 2R_E\hat{v}yT \frac{dn_L}{dM} \times D_S f(\mathbf{v}_{\mathbf{L}}) f(\mathbf{v}_{\mathbf{S}}) \delta^2(\hat{\mathbf{v}}(\mathbf{v}_{\mathbf{S}}, \mathbf{v}_{\mathbf{L}}, x) - \hat{\mathbf{v}}) \delta(\hat{t}(M, \hat{v}, x) - \hat{t}). \quad (2)$$

The first delta function picks out the particular $\hat{\mathbf{v}}$ while the second delta function picks out the particular \hat{t} . We convert the velocity delta function in $\hat{\mathbf{v}}$ to a delta function in $\mathbf{v}_{\mathbf{L}}$, then integrate over $\mathbf{v}_{\mathbf{L}}$ and $\mathbf{v}_{\mathbf{S}}$, and convert the second delta function to a delta function in mass:

$$\mathcal{L}(\hat{t}, \hat{\mathbf{v}}|x) = \frac{N_S 4R_E D_S y^3 T \hat{v} M \phi(M)}{\hat{t}} \frac{e^{-\left[\frac{v_L^2}{2\sigma_l^2} + \frac{v_b^2}{2\sigma_b^2}\right]}}{\langle M \rangle \rho_L 2\pi\sigma_l\sigma_b}, \quad (3)$$

where $\mathbf{v} = (v_l, v_b) = \bar{\mathbf{v}}_{\mathbf{L}} - x\bar{\mathbf{v}}_{\mathbf{S}} - y(\mathbf{v}_{\mathbf{S}} + \hat{\mathbf{v}})$, $\sigma_{l,b}^2 = \sigma_{L,l,b}^2 + x^2\sigma_{S,l,b}^2$, and l, b denote the components directed in galactic longitude and latitude, respectively. Comparing to the expression in B01, we see that the likelihood distributions agree if $\phi(M) \propto M^{-\frac{3}{2}}$. We convert from the

likelihood of a lens lying at a distance x to a likelihood in M using equation (1). We then integrate over sources at distance D_S using a model for the bulge and disk with luminosity functions measured with HST. The final constraint is to require that the main-sequence lens stars not exceed the flux limits of B01 and M02 (we ignore the contribution from red-giant lenses).

Figure 2 shows the computed mass probability for the above mass function. The white-dwarf, neutron-star, main-sequence cutoff, and black-hole mass cutoff show up as peaks in the probability distribution. The greater number of lenses at small mass compensates for the decreased probability for low \hat{v} events, biasing the probability toward smaller mass. The probability that each lens is a black hole, defined as $M > 3M_\odot$, is changed from above: 4% for MACHO-98-BLG-6, 16% for MACHO-96-BLG-5, and 76% for MACHO-99-BUL-22. MACHO-98-BLG-6 and MACHO-96-BLG-5 are most likely main-sequence or white-dwarf stars at > 4 kpc; better flux limits may rule out a main-sequence star. These probabilities change by one order of magnitude depending on β and M_{cns} , as shown in Table 1 (the labels are MACHO-XX-BLG-XX, while the first event is also OGLE-1999-BUL-32). The first two columns describe the assumed mass function, columns 3–5 give the black-hole probability for each event labeled by their MACHO event number, while the last two columns give the average of $M^{1/2}$ and M^2 for black holes divided by the average for all stars given the assumed IMF.

4. PROBABILITY OF LONG-TIMESCALE LENSING

We next compute the expected distribution of events as a function of timescale. For long timescales the a-priori differential probability distribution scales as \hat{t}^{-4} (Mao & Paczynski 1996). For solar-mass stars in the disk and bulge this behavior occurs for $\hat{t} > 200$ days. We can rescale the probability distribution for different masses

$$\frac{d^2p}{dM d\hat{t}} = \langle M \rangle^{-1} \phi(M) \frac{dp(M_\odot)}{d(\hat{t} M^{-1/2})}, \quad (4)$$

where M is measured in units of M_\odot and $dp(M_\odot)/d\hat{t}$ is the timescale probability distribution assuming all lenses have mass M_\odot . Since at long timescales $dp(M_\odot)/d\hat{t}$ scales as \hat{t}^{-4} , we can rescale this equation and integrate over mass

$$\frac{dp}{d\hat{t}} = \int_{M_1}^{M_2} \frac{d^2p}{dM d\hat{t}} dM \propto \hat{t}^{-4} \int_{M_1}^{M_2} dM \phi(M) M^2, \quad (5)$$

for $\hat{t} > M_2^{1/2} / 200$ days. The fraction of all microlensing events as a function of mass scales as $M^{1/2} \phi(M)$, while the fraction of events in the long-timescale tail scales as $M^2 \phi(M)$, strongly favoring black holes. Table 1 shows the average of $M^{1/2}$ and M^2 for black holes divided by mass-function average, showing that the fraction of black-hole events in the long-timescale tail is increased by one to two orders of magnitude as compared to the total number of events. *Thus, with a measurement of the mass distribution of events at long timescales, one can directly infer the mass function if it is independent of the location in phase space.*

Table 1: Black Hole Probabilities

β	M_{cns}	P(%)			$\langle M_{BH}^{1/2} \rangle / \langle M^{1/2} \rangle$	$\langle M_{BH}^2 \rangle / \langle M^2 \rangle$
		99-22	96-5	98-6		
2	20	97	65	30	3E-2	0.78
2	40	92	45	17	1.5E-2	0.64
2.35	20	90	33	10	7E-3	0.48
2.35	40	76	16	4	3E-3	0.26
3	20	46	4	1	5E-4	0.07
3	40	18	1	0.2	1E-4	0.02

We have computed the probability distribution for lensing by solar-mass stars (see Han & Gould 1995, 1996 for the computation technique), and then convolved with our assumed mass function to give the timescale distribution. This is compared to the observed distribution of MACHO events in Figure 3. We have binned the 252 alert events from MACHO (<http://darkstar.astro.washington.edu>) and then computed $\hat{t}^2 dn/d\hat{t}$ as $N_i \hat{t}_i^2 / (\epsilon_i \Delta \hat{t}_i)$, where i labels the number of the bin, errors are Poisson. Since the efficiencies, ϵ_i , have not been measured for the alert events, we have used the efficiency curve from Alcock et al. (2000), extrapolating to longer timescale. We note that the alert events timescales may be affected by blending and that a full analysis of efficiencies is required. The rise at long timescale may indicate that 20% underestimates the efficiency or that the longest two events are a statistical fluke. An efficiency of 100% is indicated for the the last three bins by an arrow. Decreasing β to 2 improves agreement for the shorter timescales, but the longest event still lies well above the predicted value, so it may be an improbable event.

We have tried to explain the rise at long timescale by varying the assumptions in the Galactic kinematics and density, but all reasonable modifications fail. To explain this discrepancy with a different mass function requires stars of mass $\sim 100M_\odot$ since the timescale scales as $M^{1/2}$ and the probability distribution peaks at ~ 100 days for $1M_\odot$ lenses. However, $100M_\odot$ lenses are ruled out by the $\mu-\pi$ observations which indicate that the three longest timescale events would have to be within a few hundred parsecs. This would require an even larger black hole mass density to explain the number of these events, $\sim 1M_\odot \text{ pc}^{-3}$, which exceeds the Oort limit. Also, for events near the peak of the timescale distribution for $100M_\odot$ lenses, \hat{v} should be much larger than observed.

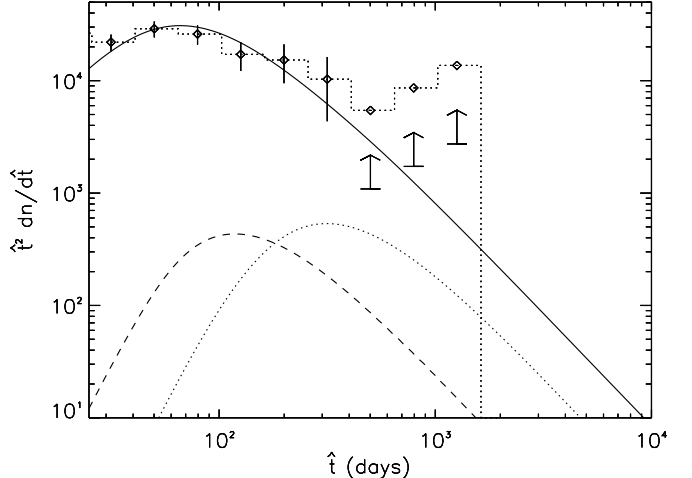


Fig. 3 - The distribution of event timescales, $\hat{t}^2 dn/d\hat{t}$.

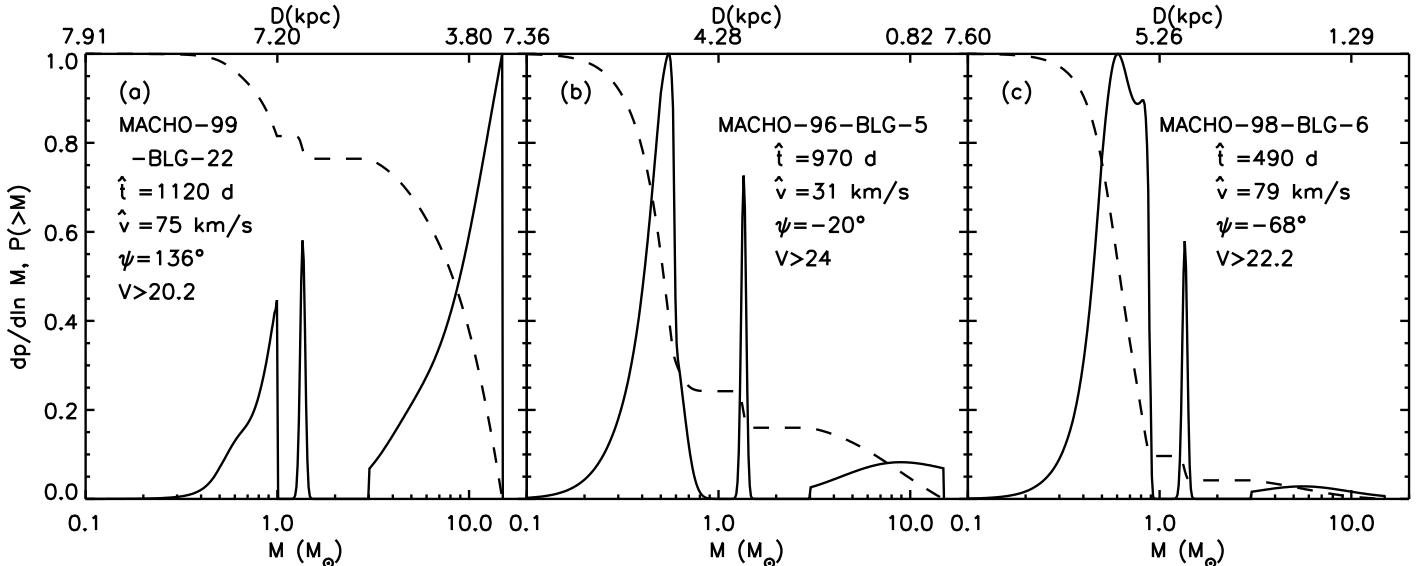


Fig. 2 - The differential (solid) and integrated (dashed) likelihood of M given the observed \hat{v} and \hat{t} . (a) MACHO-99-BLG-22 (OGLE-1999-BUL-32) (b) MACHO-96-BLG-5 (c) MACHO-98-BLG-6. The mass function parameters are $\beta = 2.35$ and $M_{cns} = 40M_\odot$. The distance scale at the top of the plots shows $D_L(M)$ if $D_S = 8$ kpc. The angle ψ is the velocity direction in Galactic coordinates measured from the rotation direction towards the north Galactic pole. The V -band flux limits are from (a) M02 (b) Bennett et al. (2002) and (c) B01.

The histogram shows the MACHO alert events, while the lines show the predicted distribution for all masses (solid), neutron stars (dashed), and black holes (dotted) for the fiducial IMF.

5. CONCLUSIONS

We have shown that including the timescale as a constraint on the black hole probability may change the conclusion as to whether or not the lens is a black hole. The probability is most robust for MACHO-99-BLG-22, which is most likely a black hole for the range of mass functions we have explored, while the probability for MACHO-98-BLG-6 and MACHO-96-BLG-5 is strongly dependent on the assumed mass function. A μ - π measurement does not provide sufficient information to estimate the mass of a given event, but may result in interesting limits on the mass.

The contribution of a given population of stars to the long-timescale tail ($\hat{t} > 200M^{1/2}$ days) of the lensing distribution depends on $\langle M^2 \rangle$ for that population. Due to their larger mass, $\sim 26\%$ of events with $\hat{t} > 600$ days should be black-hole lenses for $\beta = 2.35$ and $M_{cns} = 40M_\odot$; this fraction may be reduced if black holes have a velocity dispersion much larger than that of disk and bulge stars. To constrain β and M_{cns} with the timescale distribution will require more events and a careful estimate of the microlensing detection efficiency as a function of \hat{t} . The parallax events may have an increased efficiency since they are less affected by observing gaps and have a wider cross section due to the Earth's motion (B01).

The OGLE III project may detect 10^3 microlensing events toward the bulge each year (Paczynski, priv. comm.), which should include ~ 3 black-hole lensing events and ~ 5 neutron-star events for $\beta = 2.35$ and $M_{cns} = 40M_\odot$. Since the timescale of black-hole events

is longer, μ - π measurements are feasible from the ground (as demonstrated by B01). If these can be followed up with astrometric observations, then the mass can be determined when combined with μ - π information (Paczynski 1998, Gould 2001, Boden, Shao, & van Buren 1998). Since the typical mass of black holes, $\sim 9M_\odot$, is much higher than the typical lens mass, $\sim 0.5M_\odot$, the typical astrometric signal for black-hole lens events with a source in the bulge will be ~ 3 mas which will easily be measured with ACS (M02), VLTI (by 2004, Delplancke et al. 2001), SIM (by 2009), or GAIA (by 2010-12, Belokurov & Evans 2002), compared to 0.7 mas for a typical main-sequence lens. The deviation of the centroid is $\delta\theta = \theta_E \mathbf{u}/(u^2 + 2)$, where u is the normalized impact parameter as a function of time and θ_E is the Einstein angle (Paczynski 1998). Since u is determined by the photometric light curve, observations of $\delta\theta$ at two different u will suffice to determine θ_E . Combined with $\hat{R}_E = \hat{v}\hat{t}/2$ measured photometrically from the μ - π will allow a determination of the mass of the lens, $M = c^2 \hat{R}_E \theta_E / (4G)$. With mass measurements for many long-timescale events, the mass function can be deduced since the probability for lensing is proportional to $\hat{t}^{-4} M^2 \phi(M)$ for a phase-space distribution that is independent of mass (equation 3). The M^2 dependence means that detection of black holes will be favored so that one can constrain β and M_{cns} .

Finally, direct observations of the lenses provide another avenue toward determining their nature. If they are black holes, they may accrete from the interstellar medium or from a companion wind. With plausible assumptions, the X-ray radiation could be detectable with current space-based observatories (Agol & Kamionkowski 2001).

ACKNOWLEDGMENTS

We thank Dave Bennett and Shude Mao for constructive comments. This work was supported in part by NSF AAST-0096023, NASA NAG5-8506, and DoE DE-FG03-92-ER40701. EA was supported by NASA through Chan-

dra Postdoctoral Fellowship Award Number PF0-10013 issued by the Chandra X-ray Observatory Center, which is operated by the Smithsonian Astrophysical Observatory for and on behalf of NASA under contract NAS8-39073.

REFERENCES

Agol, E. & Kamionkowski, M., 2001, astro-ph/0109539
 Alcock, C. et al. (the MACHO collaboration), 1995, ApJ, 454, L125
 Alcock, C. et al. (the MACHO collaboration), 2000, ApJ, 541, 734
 Belokurov, V. A. & Evans, N. W., 2002, MNRAS, 331, 649
 Bennett, D. P. et al., 2001, astro-ph/0109467 (B01)
 Bennett, D. P. et al., 2002, astro-ph/0207006 (B02)
 Boden, A. F., Shao, M. & van Buren, D., 1998, ApJ, 502, 538
 Bragaglia, A., Renzini, A. & Bergeron, P., 1995, ApJ, 443, 735
 Buchalter, A., Kamionkowski, M. & Rich, M., 1997, ApJ, 482, 782
 Delplancke, F., Górska, K. M. & Richichi, A., 2001, A&A, 375, 701
 Gould, A., 2000, ApJ, 535, 928
 Gould, A., 2001, PASP, 113, 903
 Gould, A., 1992, ApJ, 392, 442
 Han, C. & Gould, A., 1995, 447, 53
 Han, C. & Gould, A., 1996, 467, 540
 Kroupa, P., 2002, Science, 295, 82
 Mao, S. et al., 2002, MNRAS, 329, 349 (M02)
 Mao, S. & Paczyński, B., 1996, ApJ, 473, 57
 Paczyński, B., 1998, ApJ, 494, L23
 Samland, M., 1998, ApJ, 496, 155
 Shapiro, S. L. & Teukolsky, S. A., 1983, Black Holes, White Dwarfs, & Neutron Stars. Wiley-Interscience, New York, NY
 van den Heuvel, E. P. J., 1992, in *Environment Observation and Climate Modeling Through International Space Projects*